Experimental and Analytical Study for Demonstration Program on Shielding of Casks for High-Level Wastes

K. Ueki[1], M. Nakazawa[2], S. Hattori[3], S. Ozaki[3], H. Tamaki[3], H. Kadotani[4], T. Ishizuka[4], S. Ishikawa[4]

[1] Nuclear Technology Division, Ship Research Institute
6-38-1 Shinkawa, Mitaka-shi, Tokyo, Japan

[2] Department of Nuclear Engineering, University of Tokyo
7-3-1 Hongo, Bunkyo-ku, Tokyo, Japan

[3] Central Research Institute of Electric Power Industry (CRIEPI)
1646 Abiko, Abiko-shi, Chiba-ken, Japan

[4] CRC Research Institute 1-3-D17 Nakase, Chiba-ken, Japan

INTRODUCTION

As a part of the safety demonstration tests imposed on a cask for high-level wastes, shielding experiments have been performed at the Central Research Institute of Electric Power Industry (CRIEPI) under contract with the Science and Technology Agency (STA) of Japan. The objective of the study is to validate the shielding ability of the demonstration-test cask for high-level wastes transport and to decide whether or not the cask is satisfied with the dose levels prescribed by the IAEA safe transport regulations (IAEA 1985).

The cask provided for the demonstration tests was designed to contain twenty eight canisters for vitrified high-level wastes. The main shield for gamma rays is a thick carbon steel, and for neutrons a thick silicone rubber layer. Outside of the silicone rubber, a thin carbon steel layer covers it completely to shield secondary gamma rays mainly produced in it.

Whenever possible, a shielding test for a high-level wastes transport cask should use actual vitrified wastes as the radiation source. However, radiation protection and handling of such radioactive materials are very difficult at the CRIEPI experimental facility, so the shielding experiments were carried out with a ^{60}Co source for gamma-rays and a ^{252}Cf source for neutrons. The shielding test was carried out prior to other tests. Gamma ray and secondary gamma-ray dose equivalent rates were measured in detail by an ionization-chamber type survey meter and neutron dose equivalent rates were measured by a moderator-type dosimeter to obtain the dose equivalent rate distributions in the cask areas of interest.

The experiments have been analyzed by the discrete-ordinates code DOT 3.5 (Mynatt et al. 1969, DOT 3.5 1975) and the continuous energy Monte Carlo code MCNP (Bricsmeister (ed.) 1986). In this study, the next event surface crossing (NESX) estimator for cylindrical surface detectors was investigated and the subroutine TALLYD was revised so as to do the present Monte Carlo calculations with the NESX estimator. Most of the Monte Carlo calculations, the results with the NESX estimator can be expected to have smaller FSDs (fractional standard deviation) than those of the usual point detector or surface crossing estimators (Ueki et al. 1981, 1983, 1990). The MCNP code was employed primarily for the neutron transport calculations and the DOT 3.5 for the gamma-ray calculations.

OUTLINE OF SHIELDING EXPERIMENT

Cask Provided for the Experiment

The cask made for the demonstration tests is able to load twenty eight canisters of vitrified high-level wastes. However, the gamma-ray source employed in the experiment was ^{60}Co distributed uniformly on the surface of cylindrical shell and the neutron source was ^{252}Cf. As illustrated in Fig.1, the cask structure has the following features:

1. The aluminum basket in which twenty eight canisters are loaded is set in the core of the cask. However, the basket with the canisters removed from the core and the cylindrical surface source of 50 cm^{ϕ} $\times$50 cm is moved from the bottom to the top in the core during the shielding experiments.
2. The outside of the core is surrounded by a thick carbon steel layer to shield mainly gamma rays and also to protect the cask against the special conditions defined by the IAEA regulations.
3. A silicone rubber layer with boron is provided to shield mainly neutrons penetrated through the carbon steel layer.
4. Outside of the silicone rubber, a thin carbon steel layer covers completely the silicone rubber to shield secondary gamma-rays produced mainly in the silicone rubber and also protect against normal conditions defined by the IAEA regulations.
5. Around the trunnions, the silicone rubber shield is thinner than that of the other parts of the cask. Accordingly, it is expected that neutrons will stream through parts of the trunnions.
6. The shielding test facility has a thick concrete floor and walls, and a thin iron ceiling. Thus the dose equivalent rate distributions are affected by room scattered radiations. Accordingly, those room-structures have to be included in the shielding analysis.

Radiation Sources

The cask shielding experiment should employ, whenever possible, actual vitrified high-level wastes as the gamma ray and neutron sources. However, in consideration of radiation protection and handling, such strong sources cannot be used in the CRIEPI facility, therefore the following sources were used in the experiment:

1. Cobalt-60 with a half-life of 5.27 y was the gamma-ray source and californium-252 with a half-life of 2.65 y was the neutron source.
2. Intensity of the gamma-ray source was 2.26×10^{12} p/s and the neutron source was 2.02×10^{9} n/s. Both sources were made up of 80 particles. Those particles were distributed on the surface of a midair cylindrical shell of 50 cm^{ϕ} $\times$50 cm.
3. The neutron energy spectrum of the ^{252}Cf source is simulated by the following equation:

$$N(E) \sim e^{-0.88E} \sinh\left[(2.0E)^{1/2} \right] \qquad (1)$$

where E is the neutron energy in MeV.

Measurements

Neutron, secondary and primary gamma-ray dose equivalent rates were measured in detail to obtain the dose equivalent rate distributions in the cask areas of interest.

The detector for measuring neutron dose equivalent rates was a moderator-type dosimeter made by Studsvik of Sweden; secondary and primary gamma-rays were measured with an ionization-chamber survey meter by Aloka of Japan. Conversion of pulses obtained from the neutron dosimeter into a neutron dose equivalent rate was by the factor of 3.03 count/s = 10 μSv/h. The value of 3.03 is from a calibration with a ^{252}Cf source. The neutron dosimeter with a polyethylene cylinder had a 21.2 cm radius and was 23.2 cm high; the survey meter with an ionization chamber had a 15 cm radius and was 10 cm high. The effective center of the detector was assumed to be 10 cm inside for the

neutron dosimeter and 5 cm inside for the gamma-ray survey meter. The cask was set upright at the center of the turntable in the shielding test facility, as shown in Fig. 2, and two-types of experiments were carried out for gamma rays and neutrons:

Type1. The source was moved parallel to the detector in ten steps by an interval of 50 cm in height in the axial direction, that is, the center of the source is at the same level as the detector.
Type2. The source was moved from the bottom to the top in ten steps, but the detector was fixed at the specified height. Then the detector was moved to several points in the radial direction.
The type 1 experiment was to obtain the dose equivalent rate distributions in the axial direction; the type 2 experiment was in the radial direction.

Future Experiment Program for Neutrons

As illustrated in Fig.2, the cask has a large cavity in which the neutron source is moved from the bottom to the top. There are some steel structures around ceiling at the cask top. In addition to a steel turntable and a concrete floor existing under the bottom of the cask. Accordingly, when the neutron source is set at the upper site or the lower site in the cask cavity, a number of neutrons scattered from those structures come into the neutron dosimeter as room scattered neutrons. Therefore, as shown in Figs 1 and 2, to reduce those obstructive neutrons and to measure the neutrons just from the cask as much as possible, a plan has been made to set up a water tank with boronic acid solution at the top and also a water layer at the bottom in the future shielding experiment program.

It is expected that the shielding effect of the water layer settled at the bottom will be more noticeable than that of the water tank against the obstructive neutrons. Accordingly, as a preliminary survey, the shielding effect of a water layer with 5 w/o boronic acid solution at a 30 cm height was estimated by the MCNP calculation.

CALCULATION TECHNIQUES

DOT 3.5 Calculation

The two-dimensional discrete ordinates code DOT 3.5 was employed to calculate the gamma-ray experiment. Not only the cask but also the floor and concrete walls, the steel turntable and ceiling were taken into account in the DOT 3.5 calculations. A cross-section library SLJ-37 was used in the DOT 3.5 calculations. A new SLJ-37 library was produced by averaging VITAMIN-C (DLC-41) (Roussin et al. 1978) cross sections with the ANISN code. The new library is composed of 36 groups for neutrons and 18 groups for the neutron's coupled cross sections, and the Legendre expansion coefficient is truncated by P_3 .

MCNP Calculation

Selection of the estimator is one of the most important things to obtain reliable results with small FSDs effectively in the Monte Carlo calculations. Many studies on the estimators have reported that smaller FSDs can be expected in the Monte Carlo calculations with the NESX estimator than those with other estimators (collision density, track length, surface crossing, and point detector estimators). However, the NESX estimator is not coded in the estimation subroutine TALLYD of the original MCNP code. Hence, the TALLYD was revised and the NESX estimator was incorporated into the revised TALLYD of the MCNP code.

In the NESX estimator, particles emerging from a collision site are examined whether or not they cross the surface detector. The probability that a particle emerging from a collision site will cross the surface before its next collision is zero if there is no detector along the path; the probability is $e^{-\eta}$ if the path is toward the surface detector. The configuration of the NESX estimator employed

in this study is illustrated in Fig.3. Several cylindrical surface detectors were located as the NESX estimators in the cask areas of interest. As shown in Fig.3, if the collision site is in the cask shield, the contributions to the detector is one or zero; if the site is in the facility structure, the contributions are two, one, or zero.

$$\Psi = W \cdot e^{-\eta} \cdot | \overline{n} \cdot \overline{\Omega} |^{-1} \cdot A^{-1} \quad , \qquad (2)$$

where

Ψ = contribution of the fluence per collision
W = weight of the particle
A = area of the surface detector
$\overline{\Omega}$ = unit direction vector of the particle
$\overline{n}$ = unit vector normal to the surface at the point where the particle crosses
η = mean-free-path between the collision site and the crossing point on the detector.

On the other hand, the fundamental and powerful tool for increasing particle collision density not only in the outer shields of the cask but also in the facility structures, the weight window importance sampling technique was employed in the MCNP code. Increasing the collision density contributes directly to a reduction in the FSDs and also leads to reliable Monte Carlo calculations. In order to determine the weight window importance parameters based on an empirical formula, the thick carbon steel, the silicone rubber and other shields were finely divided, that is, each divided iron cell was 8.5 cm thick, silicone rubber cell was 7.0 cm thick, and the water layer with boronic acid solution was 10 cm thick. Also the energy regions were divided into three intervals, that is $0.025\ eV < En \leqq 0.001$, $0.001 < En \leqq 0.1$, and $0.1 < En \leqq 15$ MeV.
The boundary energies were determined as follows :
(i) 0.001 MeV = dose conversion factor below this energy is almost constant,
(ii) 0.1 MeV = lower limit of the fast neutron,
(iii) 15 MeV = the maximum energy of spontaneous fission neutrons from ^{252}Cf.

On the other hand, the weight window importance parameters were obtained from the following empirical formula in each divided cell:

$$Wm = Wo \cdot f^{m-1} \qquad (3)$$

where Wm: lower weight bound in the m-th cell, the order of m was assigned from the cavity to the outer shields,
Wo: initial value of the weight bound,
f: a factor of which depends on energy, material and thickness.

In the present cask shielding calculations, the parameter " f " in Eq.(3) was determined by basing the dose equivalent rate attenuation experiments with a ^{252}Cf source for several materials (Ueki et al. 1992). The following values were actually employed:
(i) Thermal $< En \leqq 0.001$ MeV, Wo = 1.0 f = 0.75 for 8.5 cm thick steel, 0.5 for 15.0 cm thick concrete, 7.0 cm thick silicone rubber and 10 cm thick water with boronic acid solution,
(ii) $0.001 < En \leqq 0.1$ MeV, Wo = 0.75 f = 0.75 for steel, 0.2 for concrete, silicone rubber and the water layer,
(iii) $0.1 < En < 15$ MeV, Wo = 0.5 f = 0.5 for steel, 0.1 for concrete, silicone rubber and the water layer.

Applying the above Monte Carlo techniques, the FSDs of all the present MCNP calculations were between 0.03 and 0.08; where FSD < 0.1, the Monte Carlo result is decided as reliable (Bricsmeister (ed.) 1986). The facility structures such as the ceiling, turntable walls, and floor were taken into account in the MCNP calculations as detailed as possible. Atomic number density of the shielding materials are summarized in Table 1.

Table 1 Atomic Number Density of Shielding Materials

Element	Material (atoms / barn · cm)						
	Silicone Rubber	Carbon Steel	Air	FF Paper	Concrete	SUS 304	Water
Hydrogen	3.788×10^{-2}				1.344×10^{-2}		6.625×10^{-2}
Carbon	7.821×10^{-3}	1.183×10^{-4}			1.128×10^{-4}		
Boron	1.454×10^{-3}						
Nitrogen			4.198×10^{-5}				
Oxygen	2.989×10^{-2}		1.120×10^{-5}	5.672×10^{-3}	4.488×10^{-2}		3.313×10^{-2}
Magnesium					1.210×10^{-4}		
Aluminum	5.937×10^{-3}			1.736×10^{-3}	1.702×10^{-3}		
Silicon	7.783×10^{-3}	3.759×10^{-4}		1.534×10^{-3}	1.626×10^{-2}	1.683×10^{-3}	
Sodium					9.430×10^{-4}		
Potassium					4.505×10^{-4}		
Calcium					1.471×10^{-3}		
Chromium						1.636×10^{-2}	
Manganese		1.162×10^{-3}				1.721×10^{-4}	
Iron	9.058×10^{-5}	8.303×10^{-2}				6.010×10^{-2}	
Nickel					3.209×10^{-4}	6.444×10^{-3}	

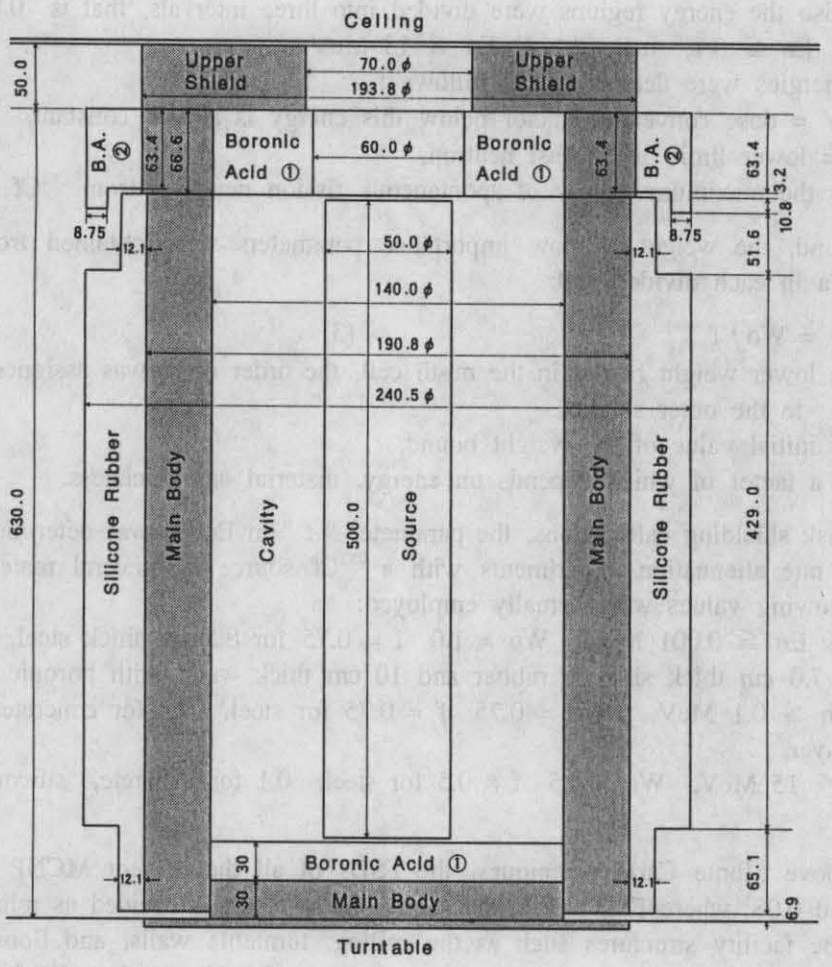

Fig.1 Calculation model of the high-level wastes transport cask in the Monte Carlo analysis. Dimensions are all in centimetres.
① In future establishment ② existing

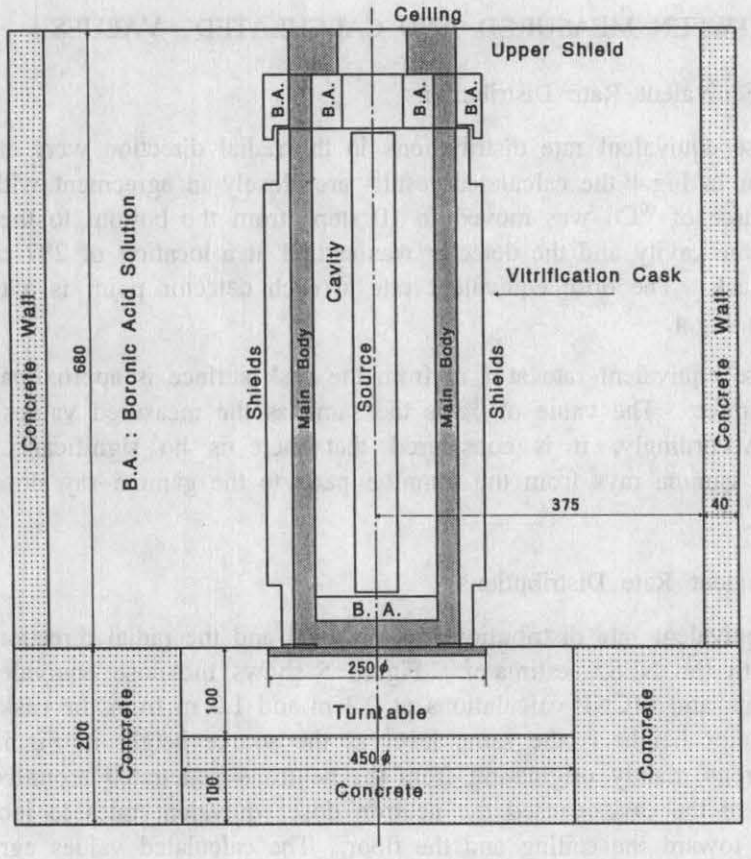

Fig.2 Calculation model of the cask and the experimental facility in the Monte Carlo analysis. Dimesions are all in centimetres.

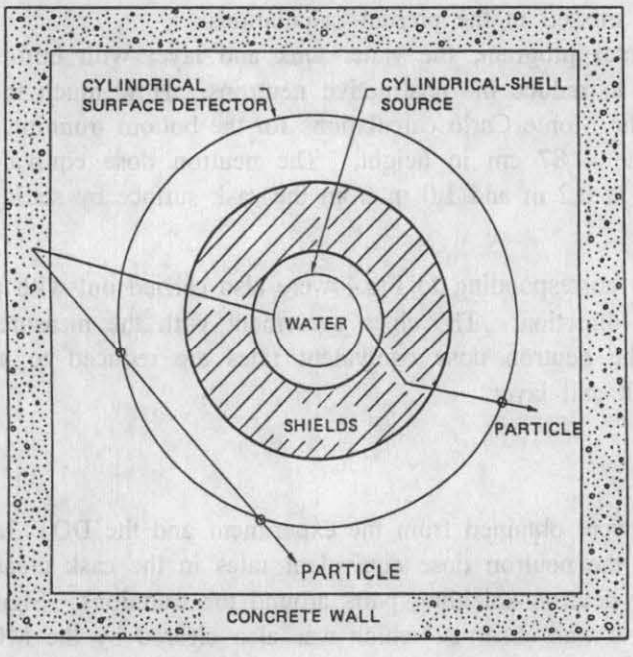

Fig.3 Illustration of the NESX estimator in analysis of the cask shielding experiment.

COMPARISON BETWEEN MEASURED AND CALCULATED VALUES

Gamma-ray Dose Equivalent Rate Distributions

The gamma-ray dose equivalent rate distributions in the radial direction were analyzed by the DOT 3.5 code. As shown in Fig.4 the calculated results are closely in agreement with the measurements. The gamma-ray source of ^{60}Co was moved in 10 steps from the bottom to the top by intervals of 50 cm in height in the cavity and the detector was settled at a location of 287 cm in height; that is, the middle of the cask. The dose equivalent rate at each detector point is a total of the 10 steps source movement in Fig.4.

The gamma-ray dose equivalent rate at 1 m from the cask surface is approximately one-half at 0.2 m from the cask surface. The value of ½ is the same as the measured values ones for spent fuel transport casks. Accordingly, it is considered that there is no significant contribution of the obstractive scattered gamma rays from the trunnion parts to the gamma-ray dose equivalent rates in Fig.4.

Neutron Dose Equivalent Rate Distributions

The neutron dose equivalent rate distributions in the axial and the radial directions were analyzed by the MCNP code with the NESX estimator. Figure 5 shows the dose equivalent rate distributions between measurements and MCNP calculations at 0.2 m and 1.0 m from the cask surface in the axial direction. The detector height is the same level as the source height in Fig.5. As expected, the room-scattered neutrons mainly originating from the neutrons penetrated around the trunnions at the top and the bottom of the cask, caused the neutron dose equivalent rates to increase rapidly as the detector was moved toward the ceiling and the floor. The calculated values agreed fairly well with the measured ones when the detector was at the middle of the cask, i.e., the detector = source = 287 cm in height. However, the calculations indicate significant underestimations when the detector was at the highest and the lowest levels. One of the promising reasons for the underestimation is that some complicated structures making the scattering of a number of neutrons which contribute to the detector locations were missed in the present calculations.
In the future experimental program, the water tank and layer with boronic acid will be set up as shown in Figs.1 and 2 to reduce the obstructive neutrons. How much the neutrons can be reduced was also estimated by the Monte Carlo calculations for the bottom trunnion part and indicated in Fig.5 at the detector = source = 87 cm in height. The neutron dose equivalent rates were reduced to approximately 1/4~1/5 at 0.2 m and 1.0 m from the cask surface by setting up the boronic acid tank and layer.

The MCNP calculations corresponding to Fig.4 were also carried out with and without the water tank and layer in the radial direction. The close agreement with the measured values was obtained as shown in Fig.6, and the neutron dose equivalent rates are reduced to approximately one-half by preparing the water tank and layer.

CONCLUSIONS

The following remarks were obtained from the experiment and the DOT 3.5 and the MCNP analyses on the gamma ray and the neutron dose equivalent rates in the cask areas of interest.
1. The cask has thinner neutron shielding parts around the trunnions. Significant neutrons streaming around the trunnion parts was observed which was also cleared by the MCNP analysis for the ^{252}Cf source experiment. Accordingly, detailed neutron streaming calculations are required to evaluate the dose levels around the trunnions when loading the vitrified high-level wastes.
2. The room-scattered obstructive neutrons, mainly originating from the neutrons penetrating around

the trunnions, at the top and the bottom of the cask are reduced significantly by preparing the water tank at the top and the water layer at the bottom. Therefore, a more accurate experiment is to be carried out in the future shielding experiment especially for neutrons. However, because the water tank and the layer do not exist in the actual high-level wastes transport cask, the experiment without the water tank and layer are not dispensable to demonstrate the transport conditions of the actual cask, too.

3. The gamma-ray and the neutron dose equivalent rate distributions obtained from the DOT 3.5 and the MCNP calculations, respectively, agreed closely with the measured values in the cask areas of interest. Accordingly, the DOT 3.5 code and the MCNP code with the NESX estimator can be employed not only for the shielding analysis of the future experiments, but also for making a safety analysis report of high-level wastes transport casks.

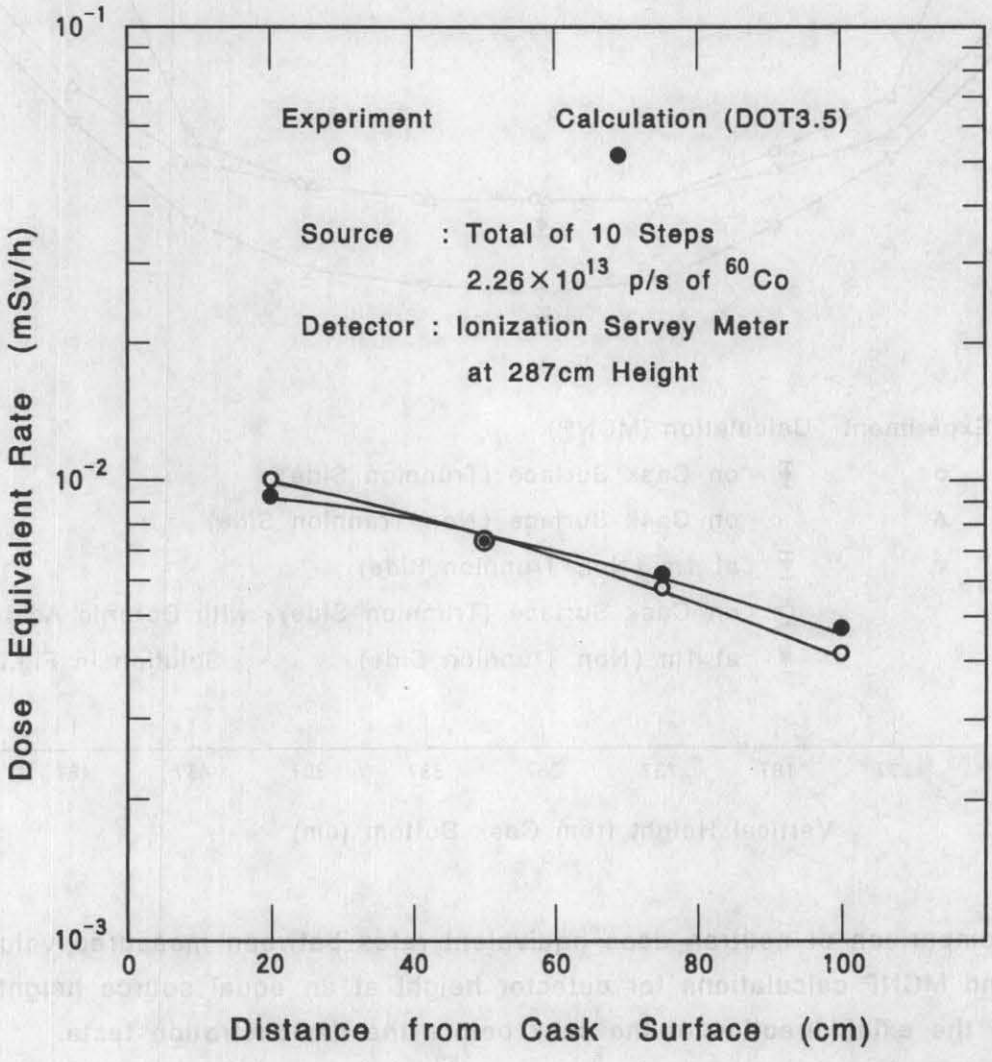

Fig.4 Comparison of gamma-ray dose equivalent rates between measured values and DOT 3.5 calculations in the radial directions of the cask before the demonstration tests.

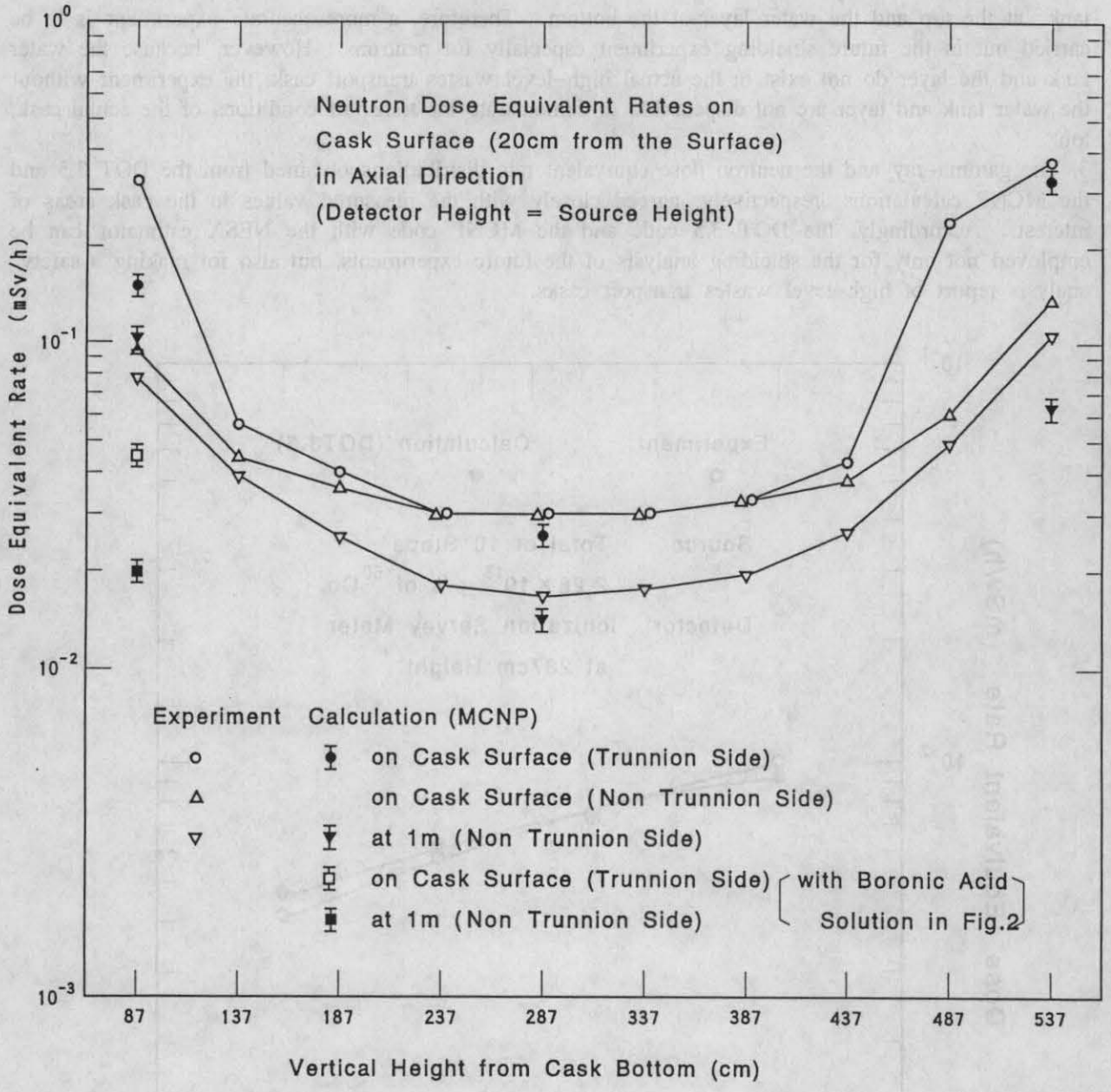

Fig.5 Comparison of neutron dose equivalent rates between measured values and MCNP calculations for detector height at an equal source height in the axial direction of the cask before the demonstration tests. Source intensity is 2.02×10^{9} n/s of ^{252}Cf at each step.

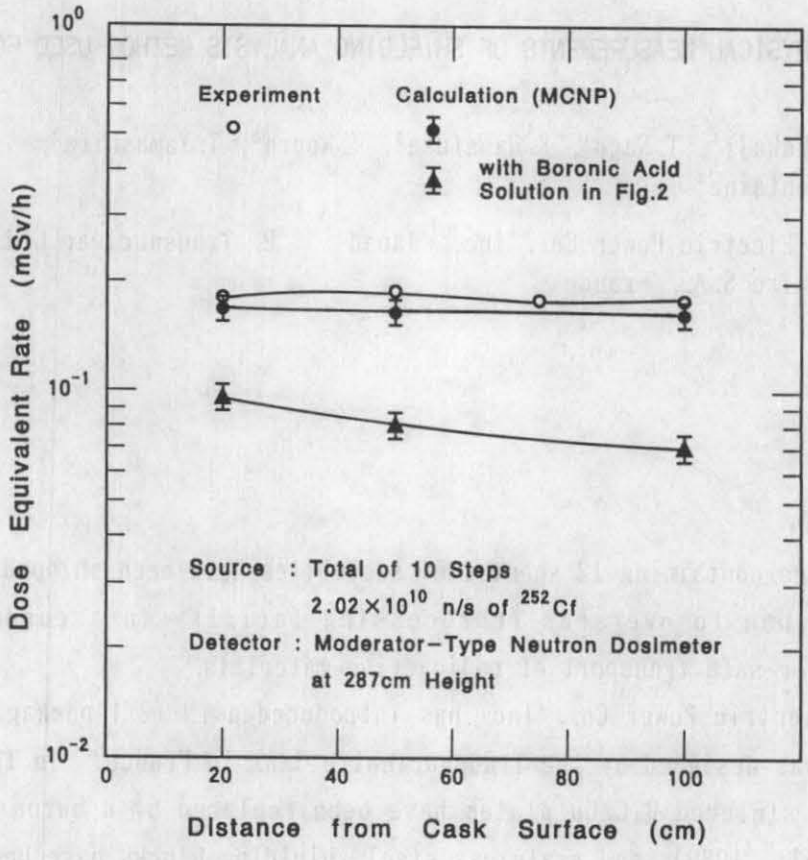

Fig.6 Comparison of neutron dose equivalent rates between measured values and MCNP calculations in the radial directions of the cask before the demonstration tests.

REFERENCES

IAEA Safety Standards, Regulations for Safe Transport of Radioactive Materials, 1985 Edition, International Atomic Energy Agency (1985).

Mynatt, F. R., Muckenthalear, F. J., and Stevens P. N. Development of Two-Dimensional Discrete Ordinates Transport Theory for Radiation Shielding, CTC-INF-952, Union Carbide Corporation, Nuclear Division (1969) ; see also, DOT 3.5, Two-Dimensional Discrete Ordinates Radiation Transport Code, RSIC Computer Code Collection CCC-276, Oak Ridge National Laboratory (1975).

Roussin, R. W., et al. VITAMIN-C : The CTR Processed Multigroup Cross-Section Library for Neutronics Studies, ORNL/RSIC-37 (ENDF-296), Union Carbide Corp., Nuclear Division, Oak Ridge National Laboratory (1978).

Bricsmeister, J. F., (ed.) MCNP-A General Monte Carlo Code for Neutron and Photon Transport, LA-7396-M, revised 2 (1986).

Ueki, K. Three-dimensional Neutron Streaming Calculations Using the Monte Carlo Coupling Technique, Nucl. Sci. Eng., 79. 253 (1981).

Ueki, K., Inoue, M., and Maki, Y. Validity of the Monte Carlo Method for shielding Analysis of a Spent-Fuel Shipping Cask : Comparison with Experiment, Nucl. Sci. Eng., 84. 271 (1983).

Ueki, k. Application of the Monte Carlo Method for Neutron Shielding Analysis of Transport Casks, Int. J. RAMTRANS, 1. 169 (1990).

Ueki, K., et al. Neutron Shielding Ability of KRAFTON N2-Mannan-KRAFTON N2 Sandwich-Type material and Others, Proceedings of the Topical Meeting on New Horizons in Radiation Protection and Shielding, American Nuclear Society, Pasco, Washington (1992).